ISSN 0001-4338, Izvestiya, Atmospheric and Oceanic Physics, 2011, Vol. 47, No. 5, pp. 572–583. © Pleiades Publishing, Ltd., 2011.
Original Russian Text © S.A. Sorokina, I.N. Esau, 2011, published in Izvestiya AN. Fizika Atmosfery i Okeana, 2011, Vol. 47, No. 5, pp. 622–633.

Meridional Energy Flux in the Arctic from Data of the Radiosonde Archive IGRA

S. A. Sorokina and I. N. Esau

Nansen Environmental and Remote Sensing Center, Bjerknes Center for Climate Research, Bergen, Norway

e-mail: svetlana.sorokina@nersc.no

Received May 13, 2010; in final form, August 2, 2010

Abstract—The meridional energy transport into high latitudes of the Northern Hemisphere is an important climate-forming factor in the Arctic. This work presents the results of calculating the meridional energy flux across 70° N based on the Integrated Global Radiosonde Archive (IGRA) data from the radio sounding of the atmosphere. The long-term mean energy flux over the period 1992–2007 in the layer from the Earth's surface to 30 hPa is 70.6 W m^{-2}. The fraction of the sensible heat flux is 23.2 W m^{-2}, i.e., 33% of the total energy flux; the fraction of the latent heat flux is 28.0 W m^{-2} (40% of the total energy flux); the fraction of the potential energy is 20.0 W m^{-2} (27%); and the fraction of the kinetic energy is 0.53 W m^{-2}, i.e., less than 1% of the total energy flux. The vertical structure of the flux shows that the main energy transport into the Arctic takes place in the middle troposphere–lower stratosphere layer, whereas the energy is transported mainly out of the Arctic in the lower troposphere, which agrees well with the schematic notion about the polar circulation cell. The spatial structure of the flux shows that the key regions with a positive (directed into the Arctic) energy flux are located in the vicinity of 160° E (the northwestern part of Eurasia, Pacific sector) and 50° W (Greenland sector). The regions with a negative (directed out of the Arctic) energy flux are located near 120° W (Canadian Arctic Archipelago) and from 20° E to 90° E (Atlantic sector). In the period from 1992 to 2007, the meridional energy transport into the Arctic weakened by −0.26 W m^{-2} yr^{-1}. The changes were mutually correlated; namely, positive and negative energy fluxes weakened in amplitude, almost without changing their locations.

Keywords: dynamics of the atmosphere, meridional transport, the Arctic.

DOI: 10.1134/S0001433811050112

1. INTRODUCTION

Any regional climatic system depends on the transboundary energy exchange. For the Arctic climatic system, the transboundary energy exchange is one constitutive factor for climate formation. For definiteness, let us designate the Arctic as a region bounded by 70° N on the south, which approximately coincides with the boundaries of the Arctic Ocean (Fig. 1).

Transboundary meridional energy fluxes across 70° N (MEF70s) have been analyzed by many authors. MEF70 calculations were based on both data from an objective analysis of observations [1–3] and from models and reanalysis [4–8]. These works will be considered below and compared with the calculations based on the Integrated Global Radiosonde Archive (IGRA) data from radio sounding of the atmosphere.

One of the first estimates of energy-flux variations across 70° N was proposed in work [1]. For the MEF70 calculation, the authors of the cited work used the Geophysical Fluid Dynamic Laboratory (GFDL) statistical data on the global atmospheric circulation over 1963–1973 based on an objective analysis of observations, mainly on the data of radio sounding of the atmosphere. It was revealed in subsequent investigations that the meridional energy flux into the Arctic has a clearly pronounced annual cycle with a minimum in summer and a maximum in winter [4, 9]. The main contribution to the meridional energy flux is made by sensible heat, potential energy, and latent heat [1, 5]; however, the quantitative estimates of these components differ by more than 20% if different data sources are used [1, 5]. The kinetic energy flux amounts to less than 1% of the total energy flux [5] and is often disregarded in calculations [1–3, 5, 6].

There is a reason latitude 70° N was chosen for calculations. As is shown in work [10], at 70° N, models predict the strongest linear relation (correlation) between the Arctic climates presented by the surface air temperature and the meridional energy flux. In addition, the boundary 70° N largely coincides with the boundary of the region of influence of the circular stationary mode of the high-latitude climatic variability known as the Arctic Oscillation [11, 12].

It is generally acknowledged that the meridional energy flux is one of the main mechanisms of sustaining the energy balance of the Arctic. The facts supporting the predominant MEF70 influence on the tropospheric climate in the Arctic are presented in a

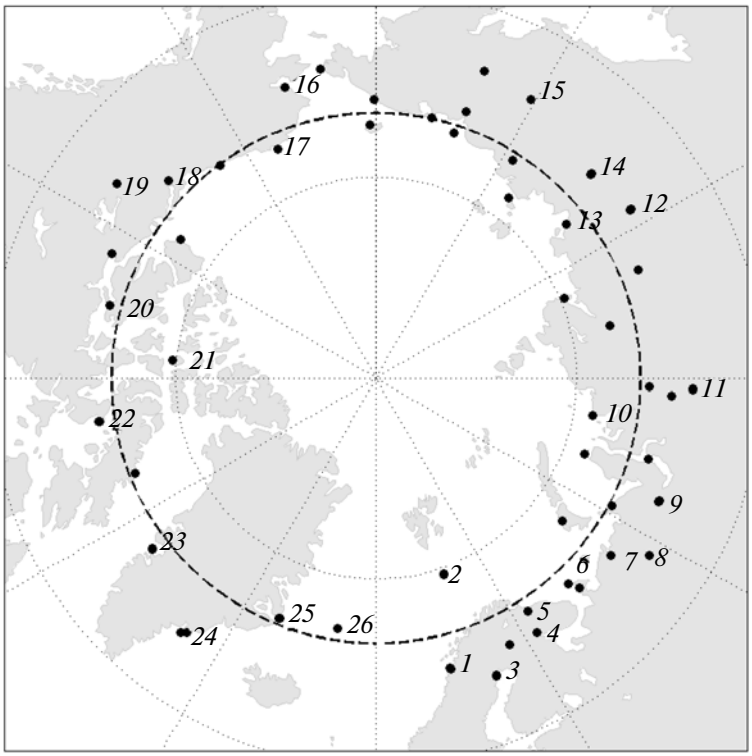

Fig. 1. Map showing the positions of the radio-sounding stations whose data are used in this work. The dashed line is drawn along the latitude 70° N. Data from the numbered stations, which were selected in accordance with the results of a statistical analysis of the data representativeness, are used in the calculations.

number of works [13–15]. However, quantitative estimates of this influence (compared with other mechanisms) remain a subject matter of discussion. We should preliminarily note the following. The MEF70 value and variability are largely controlled by the climate of midlatitudes through the intensity of cyclonic activity. In this case, the MEF70, due to its influence on temperature, wind, and cloudiness, controls the dynamics and climatology of sea ice in the Arctic [8]. We should also note the interrelation between the MEF70 and the Bjerknes mechanism of dynamic compensation [16] for sensible heat fluxes. This mechanism suggests that, on decadal time scales, the heat flux into the atmosphere decreases in response to the increase of such fluxes in the upper ocean layer [10, 17, 18].

Therefore, the MEF70 and its temporal variability seem to be valuable information for a complex understanding of the role of the atmosphere, cryosphere, and ocean in the formation of the climate of the Arctic and the whole globe. This work has the following structure. The initial data and the procedure of MEF70 calculation are described in Sections 2 and 3, respectively. The results of a calculation of the mean MEF70 and its comparison with the calculations of previous investigations are presented in Section 4. Section 5 is devoted to an analysis of the spatial MEF70 structure and its change from the winter to the summer season. The linear MEF70 trends are presented in Section 6.

2. INITIAL DATA

This work presents estimates of the meridional energy flux across 70° N (MEF70) over the period from 1992 to 2007. The initial data are the wind velocity and direction, air temperature, specific humidity, geopotential heights at the Earth's surface and at 15 standard isobaric surfaces 1000, 925, 850, 700, 600, 500, 400, 300, 250, 200, 150, 100, 70, 50, and 30 hPa. For estimating the meridional energy flux, we used the data from radio sounding of the atmosphere collected in the IGRA and available at [19] (checked on June 16, 2010). The IGRA archive contains data of 1485 stations distributed over the entire globe [20]; 49 of 1485 IGRA stations are concentrated near the latitude 70° N (±5°). The periods of observations are different at different stations, with the densest time series from 1970 until now [19].

For controlling the representativeness of observations, we performed a statistical analysis (checking the length and quality of the time series and estimating the vertical resolution) of the time series of 49 IGRA stations concentrated near the Arctic border. The results of estimating the vertical resolution showed that the information for the isobaric surface 925 hPa is absent

Table 1. World Meteorological Organization (WMO) aerological stations near the Arctic boundary at the latitude 70° N (±5°) selected from the results of a statistical analysis for the MEF70 calculations

no.	Station	WMO number	Latitude	Longitude	Period of observations	Number of soundings
1	Bodo	01152	14.4	67.3	1963–2008	30809
2	Bjornoya (Bear Island)	01028	19	74.5	1963–2008	31223
3	Lulea/Kallax	02185	22.1	65.6	1964–2008	36400
4	Kandalaksa	22217	32.4	67.2	1957–2008	37947
5	Murmansk	22113	33.1	69	1946–2008	47540
6	Kanin nos/Sojna	22271	43.3	68.7	1962–2008	34169
7	Narjan-Mar	23205	53.1	67.7	1963–2008	38046
8	Pechora	23418	57.1	65.1	1953–2008	43201
9	Salehard	23330	66.7	66.5	1948–2008	45131
10	Ostrov Dikson	20674	80.2	73.5	1948–2008	34768
11	Turuhansk	23472	88.0	65.8	1963–2008	37833
12	Zhigansk	24343	123.4	66.8	1950–2008	39546
13	Tiksi	21824	128.9	71.6	1948–2008	37858
14	Verkhoyansk	24266	133.4	67.5	1963–2008	33885
15	Zyryanka	25400	150.9	65.7	1954–2008	26952
16	Kotzebue	70133	197.4	66.9	1948–2008	41997
17	Barrow	70026	203.2	71.3	1948–2008	43324
18	Inuvik	71957	226.5	68.3	1963–2008	31686
19	Normann Wells	71043	233.2	65.3	1955–2008	28613
20	Cambridge Bay	71925	254.9	69.1	1970–2008	27461
21	Resolute	71924	265.0	74.7	1948–2008	44862
22	Hall Beach	71081	278.8	68.8	1957–2008	26982
23	Egedesminde	04220	307.3	68.7	1963–2008	31087
24	Angmagssalik	04360	323.3	65.9	1963–2008	30638
25	Scoresbysund	04339	338.0	70.5	1963–2008	30722
26	Jan Mayen	01001	351.3	71	1963–2008	30981

in a large number of radio soundings before 1992; therefore, for a more accurate calculation of the heat fluxes, we used only the information from 1992 to 2007. Based on an analysis of the quality of the time series, we selected 26 aerological stations (Fig.1, Table 1) near the latitude 70° N (±5°), which contained the information most valuable for our work. The data of these radio sounding stations, for the convenience of presentation and a comparison with the results of earlier works, were linearly interpolated into nodes of the regular grid with a step of 10° in longitude. However, we admit that such a method can give inaccuracies into the MEF70 estimate. It should also be noted that the use of the data obtained at the stations from band 10° can yield a certain difference in the results during their comparison with previous investigations, which were performed strictly for 70° N, due to deviations in the temperature and wind regimes at places located some distance from this latitude.

For checking the accuracy and the procedure of analyzing the IGRA data, we performed a parallel MEF70 calculation from the NCEP-1 reanalysis data [21] over a specified time period. The NCEP-1 reanalysis data are obtained with the use of the mathematical procedure of assimilation of the existing data bases with the atmospheric general circulation model [21]. As a result, most disagreements in fields of different meteorological parameters are eliminated, the data are interpolated onto a regular and finer grid in space, and the time resolution of the data improves. The NCEP-1 reanalysis has a high spatial resolution of 2.5° × 2.5° and contains information about various characteristics of the atmosphere and ocean over the period from 1948 to 2008. In this work we used the daily mean values of the wind velocity and direction, air temperature, specific humidity, and geopotential heights at the Earth's surface and standard isobaric surfaces from 1000 to 30 hPa over the period from 1992 to 2007. We reached an acceptable agreement between the MEF70 results based on the IGRA data and the NCEP-1 data processed by us. Our results also agree with independent calculations based on the reanalysis data, which were found in the published literature [4, 7, 8].

Table 2. The total MEF70 (W m^{-2}) across the vertical section of the atmosphere along 70° N calculated per unit area of the Arctic

Data source	GFDL [1]	GFDL [2]	REMO [5]	ERA 40 [6]	NCEP [4]	IGRA
MEF70	98	103	99	100	103	71

3. ANALYSIS METHOD

According to work [1], the integral meridional energy flux across the hypothetic Arctic border (MEF70) can be presented in the form

$$\mathrm{MEF70} = \iint C_p\left(\overline{\upsilon T}\right)\frac{dp}{g}dx + \iint L\left(\overline{\upsilon q_\upsilon}\right)\frac{dp}{g}dx + \iint g\left(\overline{\upsilon z}\right)\frac{dp}{g}dx + \iint\frac{1}{2}\left(\overline{\upsilon|v|^2}\right)\frac{dp}{g}dx, \quad (1)$$

where MEF70 is the energy flux across70° N (W); υ is the meridional component of the wind velocity (m s^{-1}), which is positive from south to north; q_υ is the specific humidity (kg/kg); x is the coordinate axis directed eastward along the parallel 70° N; p is the pressure (Pa); g is the gravitational acceleration, $g = 9.80665$ (m s^{-2}); C_p is the specific heat capacity of moist air at constant pressure, $C_p = 1003.5$ (J(kg K)$^{-1}$); T is the absolute temperature (K); L is the specific heat of evaporation, 2.501×10^6 (J kg^{-1}); z is the geopotential height (m); $|v|$ is the module of the wind velocity vector (m s^{-1}); the overbar means the time averaging; and () is the symbol of zonal averaging.

The right side in formula (1) contains the terms which correspond to the flows of sensible heat (enthalpy) and latent heat, potential energy, and kinetic energy. If the sum of these terms is positive, an energy flux across the specified boundary takes place; consequently, the integral MEF70 is directed into the Arctic (northward). The averaging $(\overline{\varphi})$ yields the annual mean meridional flux of the calculated characteristic φ (temperature, humidity, geopotential height, and kinetic energy). The calculations were performed separately for each atmospheric level (from the surface to 30 hPa), and then the summation along the latitudinal circle was performed for each level. At the last stage, the summation was performed for all levels with allowance for the weight of each layer $\frac{dp}{g}$. Note that, when the potential energy was found for each layer, we determined the difference Δz between the layers i and $i + 1$. Multiplied by the meridional wind velocity υ, this difference is used for calculating the mean value of the potential energy flux for each layer. For the convenience of making a comparison with the results of earlier works, the MEF70 is calculated per unit of the Arctic area located to the north from 70° N (1.5×10^{13} m^2). Therefore, the MEF70 and its components are expressed in Watts per square meter (W m^{-2}) of the area of the horizontal surface of the Arctic.

For an exact calculation of the energy flux, it is necessary that the law of the mass balance in the atmosphere be fulfilled:

$$\iint(\overline{\upsilon})\frac{dp}{g}dx \to 0. \quad (2)$$

In other words, on time scales of one month and longer, the mass flux across the Arctic boundary must tend to zero, because the mass of the atmosphere in the Arctic is approximately constant. The procedure of mass correction requires high spatial and temporal resolutions in the initial data. For using the data presented by 26 stations of radio sounding, this condition is almost impracticable due to the spatial and temporal heterogeneity of data. According to the IGRA data, the integral mass flux over the period under investigation was negative. Consequently, the MEF70 value calculated with the use of the presented radio-sounding data is underestimated because the integral mass flux is less than zero. In the previous investigations [5, 6, 24], the MEF70 value is given with allowance for the mass balance law.

4. MEAN MERIDIONAL ENERGY FLUX AT 70° N

Using the presented radio-sounding data, we calculated the annual mean climatic value of the MEF70 based on formula (1). According to the data of radio sounding of the atmosphere, the annual mean meridional energy flux is 70.6 W m^{-2} (Table 2).

An analysis of the quantitative relations of the MEF70 components obtained from radio-sounding data showed that the main contribution is made by the fluxes of latent heat (28.0 W m^{-2}), sensible heat (23.2 W m^{-2}), and potential energy (20.0 W m^{-2}), which amount to 40, 32, and 20%, respectively, of the total MEF70. The kinetic energy flux is –0.53 W m^{-2}, i.e., less than 1% of the total MEF70. Such a percentage relation of the significance of the MEF70 components agrees fairly well with the calculations presented in preceding works [1, 5, 7].

However, it should be noted that the annual mean MEF70 value obtained from the IGRA radio-sounding data was 30% smaller than the estimates of previous investigations based on the data of the GFDL objective analysis, reanalysis, and models (Table 2).

Such a difference is in compliance with the estimates obtained in [22, 23] for the meridional humidity flux, which were based on the NCEP-1 reanalysis and radio-sounding data. According to [22, 23], this difference is mainly caused by a small number or a com-

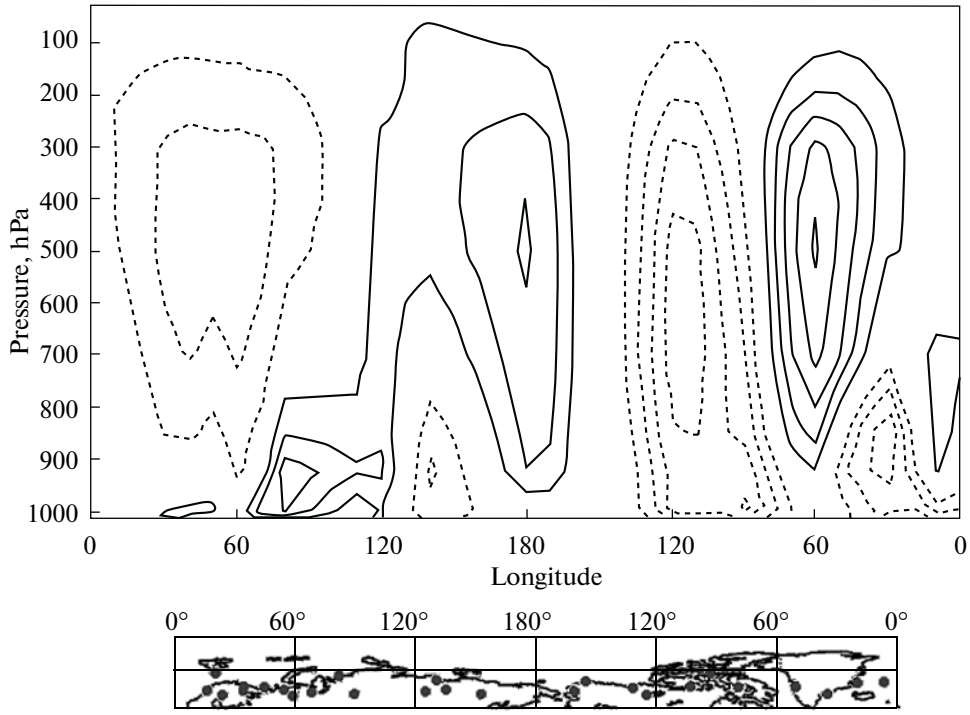

Fig. 2. Longitude–height distribution of the IGRA MEF70 values (W m^{-2}) interpolated onto the 10° longitudinal grid and averaged over the entire period from 1992 to 2007. The MEF70 contours are drawn at an interval of $|2 \times 10^5|$ (W m^{-2}). The negative MEF70 values are indicated by dashed lines. A map of adjacent territories is presented below. The IGRA stations used for calculations are marked by dots on the map.

plete absence of stations, especially in the Canadian Arctic Archipelago, Greenland, and North Atlantic regions. Additionally, the investigations performed in [24] showed that, even if the procedure of mass correction was used, the humidity fluxes at the latitude 70° N from radio-sounding data were 20% smaller than the estimates from reanalysis data due to distinctions in the spatial resolutions of data. In our case, the vertical and horizontal spatial resolutions of radio-sounding data are, respectively, 1.7 and 5.5 times smaller than for most reanalysis data, objective analysis, and model calculations. Therefore, it can be inferred that the 30% distinction of the mean MEF70 based on the presented radio-sounding data is explained by distinctions in the spatial resolution of data and by the absence of a mass balance correction in the MEF70.

5. SPATIAL STRUCTURE OF THE MERIDIONAL ENERGY FLUX AT 70° N

Figures 2 and 3 show the distributions of the mean (over the period 1992–2007) spatial structure of the MEF70 calculated from the IGRA radio-sounding data and from the NCEP-1 reanalysis data, respectively. The MEF70 has a clearly pronounced vertical structure. The maximal energy transport is observed in the middle troposphere–lower stratosphere layer. Table 3 gives the integral climatic values of the MEF70 distributed over the calculated layers. The southward (negative) energy flux with the maximal amplitude in the 925- to 1000-hPa layer, i.e., at the Earth's surface, prevails in the tropospheric layer to a height of 700 hPa. The northward (positive) energy flux with the

Table 3. MEF70 values (W m^{-2}) and linear trends (W m^{-2} yr^{-1}) for different atmospheric layers from the IGRA data

Layer thickness, hPa	Earth's surface 1000	1000 925	925 850	850 700	700 500	500 400	400 300
MEF70 (W m^{-2})	−23.9	−98.3	−71.4	−81.8	36.2	63.7	91.7
Trend (W m^{-2} yr^{-1})	0.81	1.58	−0.32	2.44	1.06	−1.00	−0.54
Layer thickness, hPa	300 250	250 200	200 150	150 100	100 70	70 50	50 30
MEF70 (W m^{-2})	41.4	21.6	15.7	24.4	20.7	16.4	13.9
Trend (W m^{-2} yr^{-1})	−0.85	−1.53	−1.34	−1.52	−0.79	−0.63	−0.97

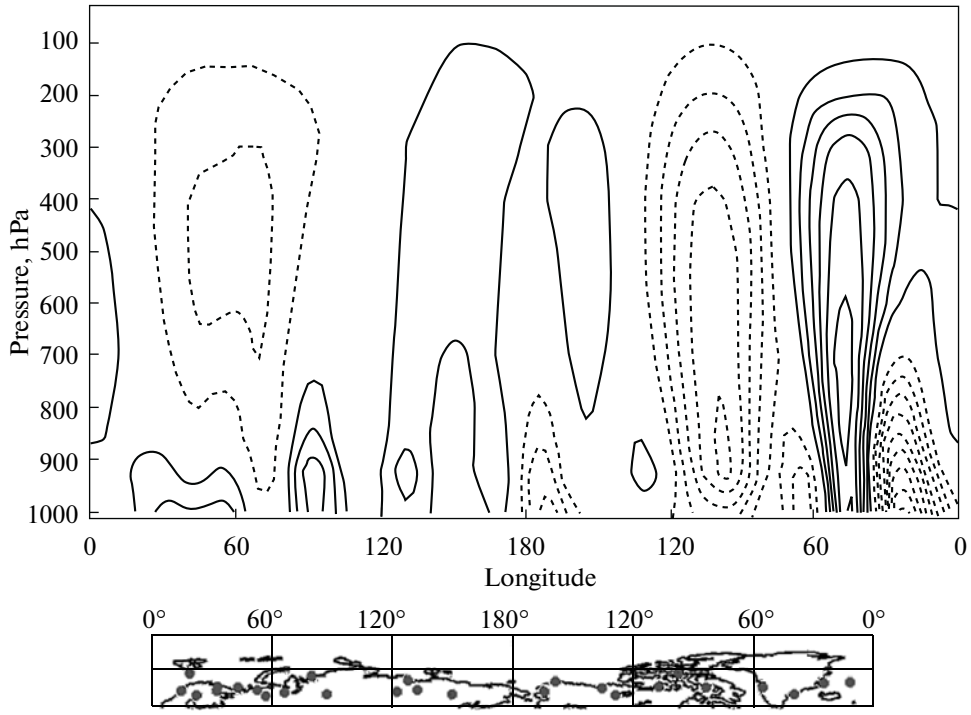

Fig. 3. The same as in Fig. 2, but for the NCEP-1 reanalysis data.

maximal amplitude in the layer from 300–400 hPa is observed beginning from the height of 700 hPa. The vertical pattern of the distribution agrees well with the previous investigations [2, 7] and corresponds to the notions about the polar circulation cell, where the northward transport takes place in the upper part of the atmosphere and the southward transport takes place near the Earth's surface.

Considering the distribution of the climatic MEF70 along the latitudinal circle, it is necessary to pay attention to the almost identical patterns obtained for the IGRA data (Fig. 2) and for the NCEP-1 reanalysis data (Fig. 3). Each atmospheric layer has a clear zonal asymmetry. According to Fig. 1, the most distinctly pronounced region of energy influx into the Arctic is located near 50° W. The flux intensifies at the height from 800 to 600 hPa. The eastern axis of the North American basin and the Icelandic low have the biggest influence on the formation of the positive flux in this region. According to Figs. 4 and 5, this flux intensifies in the cold time of the year and weakens in the warm seasons.

The region of the negative energy flux is located near 80° W. This region experiences an influence from the downward flux in the western part of the North American ridge. The flux intensity increases in winter and decreases in summer (Figs. 4, 5).

The region of the positive energy flux in the cold part of the year and the weakly negative flux in the warm part of the year is located over the eastern part of Eurasia near 160° E (Figs. 4, 5). In winter, this region experiences the influence of the northeastern branch of the Siberian high. The strong positive flux extending from 30° to 120° E in the lower troposphere (from the Earth's surface to 850 hPa) is produced due to the formation of the western branch of the Siberian high. The vast region of the negative energy flux, whose maximum varies both in longitude and during the year, is located in the middle troposphere and upper stratosphere from 30° to 120° E. This feature is explained by the predominant wind directions in the western branch of the Ural basin. The East Siberian anticyclone weakens in spring, gradually transforming into the Asiatic depression, which changes the predominant flux direction in the lower troposphere and weakens the total integral flux in this region (Figs. 4, 5). The qualitative structure of the MEF70 distribution along the latitudinal circle agrees well with the preceding works [2, 6, 7].

Figures 4 and 5 show the winter and summer MEF70 fluxes based on the IGRA and NCEP-1 data. As can be seen from these figures, the flux structure, on the whole, is retained from winter to summer. We can note the following tendency: in winter, the heat influx into the Arctic due to external factors (solar radiation and long-wave fluxes) is much smaller than at midlatitudes [6]; consequently, high gradients of temperature and pressure are formed between high and middle latitudes, leading to a high intensity of the meridional flux. In spring, the meridional energy flux considerably decreases. Beginning from February, the Arctic atmosphere is heated due to a rapid increase in

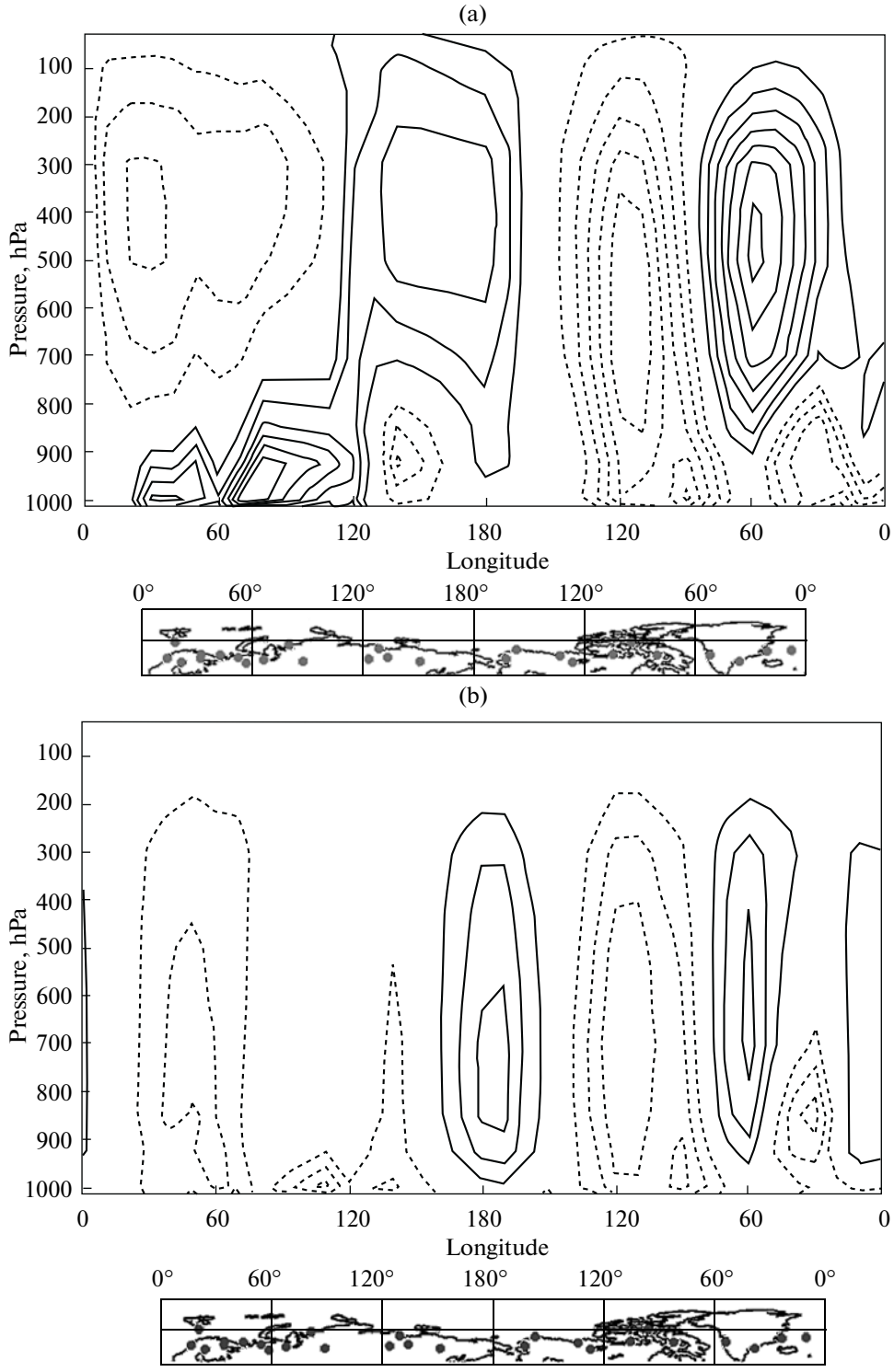

Fig. 4. Longitude–height distribution of the IGRA MEF70 values interpolated onto the 10-degree longitudinal grid (a) in the winter period from November to March and (b) in the summer period from May to September. The MEF70 contours are drawn at an interval of $|2 \times 10^5|$ (W m^{-2}). The negative MEF70 values are indicated by dashed lines. A map of adjacent territories is presented below. The IGRA stations used for calculations are marked by dots on the map.

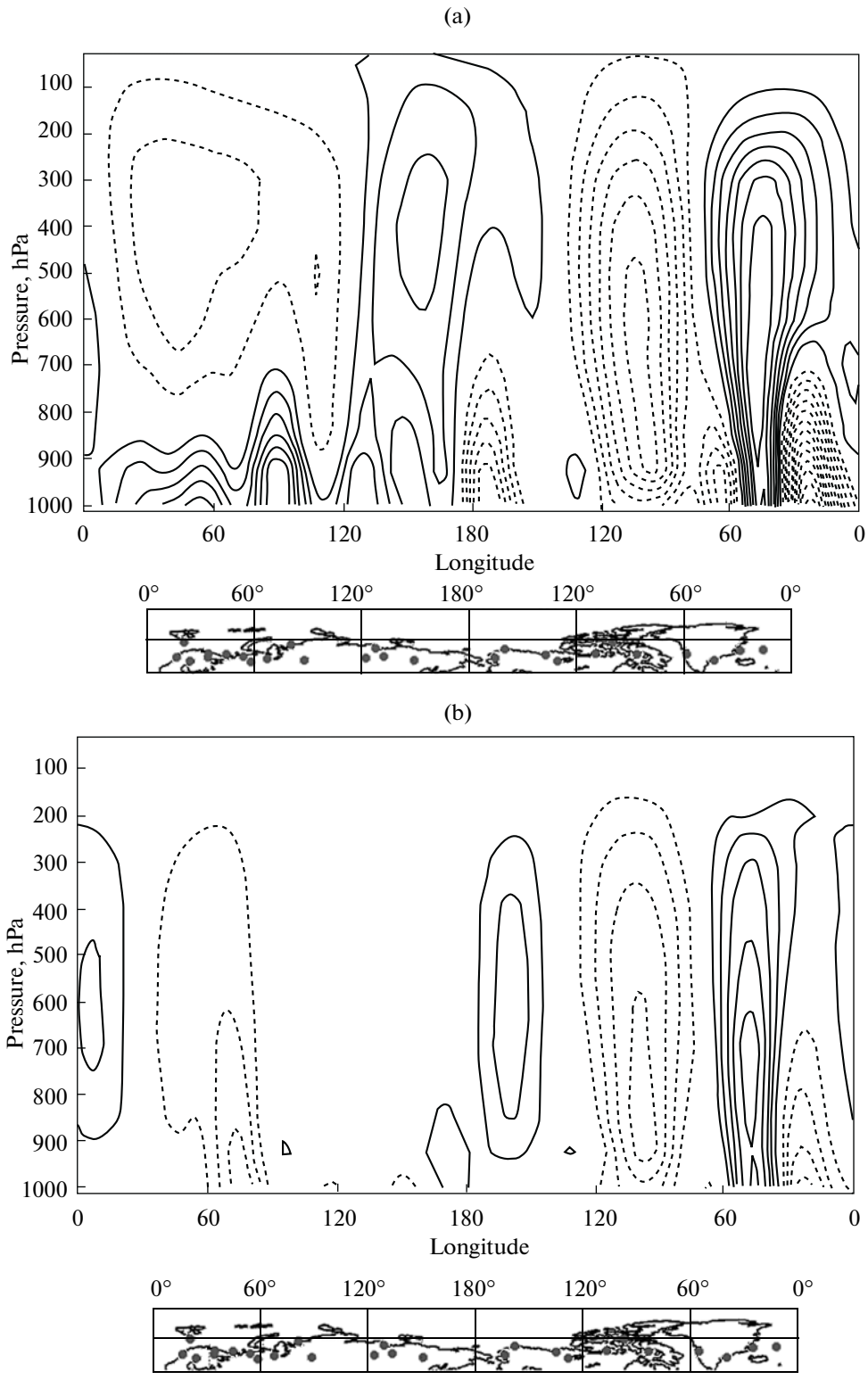

Fig. 5. The same as in Fig. 4, but for the NCEP-1 reanalysis data.

the solar radiation flux and the heat (sensible and latent) flux from the Earth's surface, and the total energy balance in the atmosphere becomes positive [6]. Consequently, the zonal mean temperature gradient between high and middle latitudes starts to decrease, which decreases the meridional flux intensity.

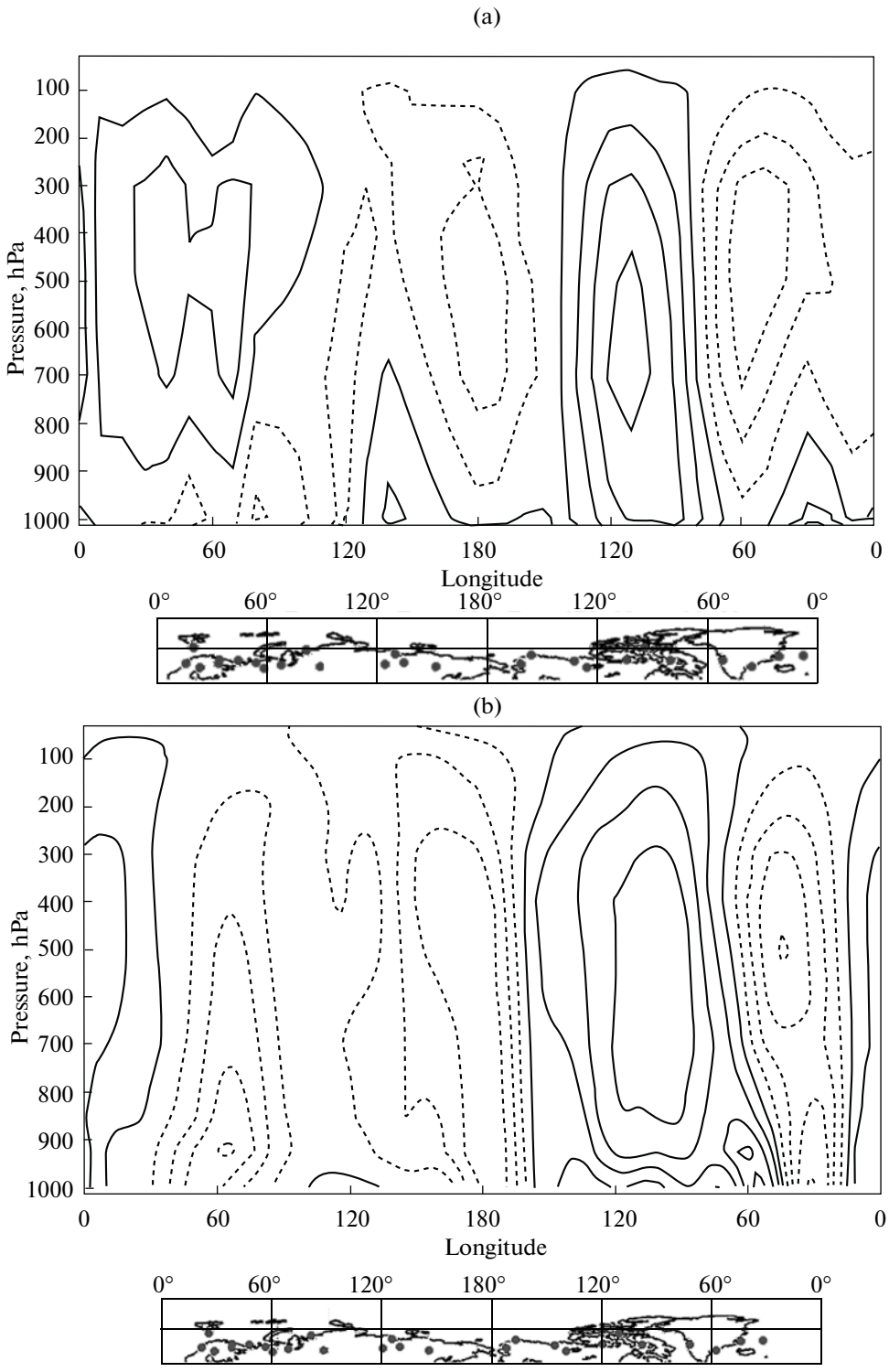

Fig. 6. Longitude–height distribution of the MEF70 linear trends (W m^{-2} yr^{-1}) interpolated onto the 10° longitudinal grid according to (a) IGRA and (b) NCEP-1 data. The contours of the MEF70 trends are drawn at an interval of $|1 \times 10^4|$ (W m^{-2} yr^{-1}). The negative MEF70 trends are indicated by dashed lines. A map of adjacent territories is presented below. The IGRA stations used for calculations are marked by dots on the map.

6. LINEAR TREND OF THE MERIDIONAL ENERGY FLUX AT 70° N AND ITS SPATIAL STRUCTURE

Considering the long-term tendencies in MEF70 variations, one can note the following. The linear trend of the MEF70 calculated from the IGRA radiosounding data for the atmospheric layer from the Earth's surface to 30 hPa is -0.26 W m^{-2} yr^{-1}, which indicates that the meridional flux into the Arctic, on the whole, becomes weaker. This tendency agrees well with the previous calculations based on the NCEP-1 reanalysis data [18], which yielded a linear MEF70 trend equal to -0.11 W m^{-2} yr^{-1} [8]. This tendency also qualitatively agrees with the results of work [7]. Table 3 gives the linear MEF70 trends over the period 1997–2007 separately for each atmospheric layer. The vertical structure of the linear MEF70 trends displays a tendency toward the weakening of the northward transport in the middle and upper troposphere and in the stratosphere and, simultaneously, a tendency toward the weakening of the southward transport in the lower troposphere.

Considering the distribution of the linear MEF70 trends along the latitudinal circle 70° N (Fig. 6), one can note the following features. During 1997–2007, the MEF70 increased in the region of the Canadian Arctic Archipelago, over the North Atlantic, and in the region of the Norwegian sea. Large negative trends were observed over northeastern Eurasia, Greenland, and in the vicinity of Novaya Zemlya Island (Barents and Kara seas). Therefore, the signs of the flux trends are, on the whole, opposite the signs of the fluxes themselves; i.e., the tendency toward the weakening of the southward flux is observed in regions where the southward flux prevails, and the tendency toward the weakening of the northward flux exists in regions with a predominant northward flux (Fig. 6). This feature points to the weakening of the meridional circulation within the polar cell as a whole. It should be noted that the redistribution of fluxes (their decrease in some sectors and increase in others) can affect the local temperature regime of the Arctic and, consequently, change the processes in the cryosphere. For example, the positive MEF70 tendency in the Atlantic sector and Europe and the negative tendency over northeastern Eurasia and Greenland must strengthen the influence of warm air from the Atlantic Ocean water areas and, on the contrary, decrease the influence of cold continental air from northwestern Eurasia and Greenland. Although further efforts are necessary for a quantitative estimation of the influence that MEF70 redistribution has on changes in the temperature regime and processes in the cryosphere, it can be supposed that this feature, which characterizes circulation variations, is one of the factors responsible for the mean temperature rise [25–25] and the substantial decrease in the ice-cover area in the Arctic [8, 28].

7. CONCLUSIONS

This work presents the spatial–temporal structure of the meridional energy flux at the latitude 70° N (MEF70) based on the IGRA radio-sounding data and its comparison with the MEF70 structure based on the NCEP-1 reanalysis data and the preceding investigations. The mean MEF70 obtained from the IGRA data over the period of 1992–2007 is 70.6 W m^{-2}, which is 30% less than the estimates obtained in the preceding investigations on the basis of the GFDL objective analysis, reanalysis, and models. Such a difference between the MEF70s is hypothetically explained by distinctions in the spatial resolutions of data and by an absence of the mass balance correction in the radio-sounding data. However, it should be noted that the quantitative estimation of the MEF70 structure according to the IGRA data correlates fairly well with the results of preceding investigations and the NCEP-1 reanalysis data.

The presented estimates of the vertical MEF70 structure showed noticeable variations in the flux distribution over height. The MEF70 has a clear vertical structure. The main energy flux into the Arctic takes place in the middle troposphere–lower stratosphere layer (700–30 hPa). In the lower atmospheric layer (to 700 hPa), the energy is predominantly carried out of the Arctic. This inference qualitatively agrees with the notions about the air circulation within the polar cell [3, 4].

An analysis of the spatial MEF70 structure shows that the key regions with the positive (directed into the Arctic) energy flux are located in the regions of 160° E (the northwestern part of Eurasia and the Pacific sector) and 50° W (the Greenland sector), whereas the regions with a negative (directed out of the Arctic) energy flux are located near 120° W (Canadian Archipelago) and from 20° to 90° E (Atlantic sector). It was shown that the cyclonic activity at middle and high latitudes substantially affects the meridional energy transport. This factor leads to an alternation of directions of the meridional energy flux at the same level. Northward fluxes prevail along some meridians, and southward fluxes prevail along other, neighboring, meridians. Distinctions between the patterns of the meridional energy fluxes in the cold and warm times of the year are noted. On the whole, the qualitative structure of the positions of positive and negative energy fluxes is retained from winter to summer. However, the following tendency is observed: due to the weakening of the zonal mean temperature and pressure gradients between high and middle latitudes in the warm time of the year, the meridional flux intensity decreases, the maxima of fluxes become smoothed, and the MEF70 field becomes more diffuse. When these gradients increase in the cold time of the year, the meridional flux intensifies and the spatial MEF70 structure becomes more contrasting.

The general tendency toward the MEF70 weakening was detected in 1997–2007. The total linear trend is –0.26 W m^{-2} yr^{-1}, which qualitatively agrees with the estimates obtained by the authors of works [7, 8]. An analysis of the spatial structure of the linear MEF70 trend showed considerable changes in the distribution of the meridional air transport between Arctic and middle latitudes over the period from 1992 to 2007. These changes manifested themselves both in the vertical distribution of the total MEF70 and in its horizontal distribution along the latitude 70° N. During 1997–2007, the MEF70 increased in the area of the Canadian Arctic Archipelago, over the Atlantic, and in the region of the Norwegian sea and decreased in the region of northeastern Eurasia, Greenland, and Novaya Zemlya Island (Barents and Kara seas). Such a redistribution of the MEF70 may enhance the influence of warm air from the Atlantic Ocean water areas and, on the contrary, reduce the influence of cold continental air from northeastern Eurasia and Greenland. It can be supposed that this feature of changes in the circulation is one of the factors responsible for the mean temperature rise [25–27] and a substantial decrease in the ice-cover area in the Arctic [27, 28].

It is necessary to note in conclusion that the question concerning the causes of the accelerated warming of the Arctic remains among the questions most hotly discussed by the world scientific community, for example, at the congress concluding the International Polar Year (Oslo, June 8–12, 2010). One of the most complex and still unclear questions is associated with the response magnitude in the MEF70 mechanism to changes in the Arctic climate. Various hypotheses predict both a decrease [10, 16] and an increase [29, 30] in MEF70. The results of our calculations, in spite of a significant uncertainty, point more likely to the MEF70 weakening in over the last few decades. Therefore, the meridional energy flux at the Arctic border and its long-term variability possibly allow us not only to understand climate changes in the Arctic itself, but also point to the mechanisms of these changes and their relation to the processes at low latitudes.

REFERENCES

1. N. Nakamura and A. H. Oort, "Atmospheric Heat Budgets of the Polar Regions," J. Geophys. Res. **93** (D8), 9510–9524 (1988).
2. J. E. Overland and P. Turet, "Variability of the Atmospheric Energy Flux across 70° N Computed from the GFDL Data Set," Nansen Centennial Volume. Geophys. Monogr. American Geophys. Union, No. 84, 313–325 (1994).
3. J. E. Overland, P. Turet, and A. H. Oort, "Regional Variations of Moist Static Energy Flux into the Arctic," J. Clim. **9** (1), 54–65 (1996).
4. K. E. Trenberth and D. P. Stepaniak, "Co-Variability of Components of Poleward Atmospheric Energy Transports on Seasonal and Interannual Timescales," J. Clim. **16**, 3691–3705 (2003).
5. T. Semmler, D. Jacob, K. H. Schlunzen, et al., "The Water and Energy Budget of the Arctic Atmosphere," J. Clim. **18** (13), 2515–2530 (2005).
6. M. C. Serreze, A. P. Barrett, A. G. Slater, et al., "The Large-Scale Energy Budget of the Arctic," J. Geophys. Res. **112** (D11122) (2007). doi: 10.1029/2006Jd008230.
7. A. A. Vinogradova, "Meridional Mass and Energy Fluxes in the Vicinity of the Arctic Border," Izv. Atmos. Ocean. Phys. **43** (3), 281–293 (2007).
8. L. H. Smedsrud, A. Sorteberg, and K. Kloster, "Recent and Future Changes of the Arctic Sea Ice Cover," Geophys. Rev. Lett. **35** (2008). doi: 10.1029/2008GL034813.
9. M. C. Serreze and R. G. Barry, *The Arctic Climate System* (UK, Cambridge University Press, Cambridge, 2005).
10. E. Van der Swaluw, S. Drijfhout, and W. Hazeleger, "Bjerknes Compensation at High Northern Latitudes: The Ocean Forcing the Atmosphere," J. Clim. **20**, 6023–6032 (2007).
11. D. W. J. Thompson and J. M. Wallace, "The Arctic Oscillation Signature in the Wintertime Geopotential Height and Temperature Fields," Geophys. Rev. Lett. **25**, 1297–1300 (1998).
12. R. Quadrelli and J. M. Wallace, "A Simplified Linear Framework for Interpreting Patterns of Northern Hemisphere Wintertime Climate Variability," J. Clim. **17**, 3728–3744 (2004).
13. M. Tsukernik, T. N. Chase, M. C. Serreze, et al., "On the Regulation of Minimum Mid-Tropospheric Temperatures in the Arctic," Geophys. Rev. Lett. **31**, L06112 (2004). doi: 10.1029/2003GL018831.
14. R. G. Graversen, T. Mauritsen, M. Tjernstrom, et al., "Vertical Structure of Recent Arctic Warming," Nature **541**, 53–57 (2008).
15. V. A. Alexeev, I. Esau, I. V. Polyakov, et al., "Vertical Structure of Recent Arctic Warming from Observed Data and Reanalysis Products," Geophys. Res. Abstr. **11**, EGU2009–11755 (2009).
16. J. Bjerknes, "Atlantic Air-Sea Interaction," Adv. Geophys. **10**, 1–82 (1964).
17. L. Shaffrey and R. Sutton, "Bjerknes Compensation and the Decadal Variability of the Energy Transports in a Coupled Climate Model," J. Clim. **19** (7), 1167–1181 (2006).
18. J. H. Jungclaus and T. Koenigk, "Low-Frequency Variability of the Arctic Climate: The Role of Oceanic and Atmospheric Heat Transport Variations," Clim. Dyn. **34**, 265–279 (2010).
19. http://www.ncdc.noaa.gov/oa/climate/igra/index.php
20. D. J. Gaffen, "A Digitized Metadataset of Global Upper-Air Station Histories," NOAA. Technical Memorandum ERL-ARL, 211.
21. Kalnay, et al., "The NCEP/NCAR 40-Year Reanalysis Project," Bull. Amer. Meteor. Soc. **77** 437–470 (1996).
22. J. L. Cohen, D. A. Salstein, and R. D. Rosen, "Interannual Variability in the Meridional Transport of Water Vapour," J. Hydromet. **1**, 547–553 (2000).
23. R. I. Cullather, D. H. Bromwich, and M. C. Serreze, "The Atmospheric Hydrologic Cycle over the Arctic

from Reanalyses. Part I. Comparison with Observations and Previous Studies," J. Clim. **13**, 923–937 (2000).

24. M. Gober, R. Hagenbrock, F. Ament, et al., "Comparing Mass-Consistent Atmospheric Moisture Budgets on an Irregular Grid: An Arctic Example," Q.J.R. Meteorol. Soc. **129**, 2383–2400 (2003).
25. "Impacts of a Warming Arctic," in *Arctic Climate Impact Assessment (ACIA)* (Cambridge University Press, Cambridge, 2004).
26. S. Kuzmina, O. M. Johannessen, L. Bengtsson, et al., *High Northern Latitude Surface Air Temperature: Comparison of Existing Data and Creation of a New Gridded Dataset 1900–2000, SCAR/IASC IPY Open Science Conf* (Russia, St. Petersburg, 2008).
27. M. C. Serreze, A. P. Barrett, J. C. Stroeve, et al., "The Emergence of Surface-Based Arctic Amplification," Cryosphere **3**, 11–19 (2009).
28. C. Deser, R. Tomas, M. Alexander, et al., "The Seasonal Atmospheric Response to Projected Arctic Sea Ice Loss in the Late Twenty-First Century," J. Clim. **23** (2), 333–351 (2010).
29. P. L. Langen and V. A. Alexeev, "Polar Amplification as a Preferred Response in an Aquaplanet GCM," Clim. Dyn. **29** (2–3), 305–317 (2007).
30. V. A. Alexeev, R. L. Langen, and J. R. Bates, "Polar Amplification of Surface Warming on an Aquaplanet in Ghost Forcing Experiments without Sea Ice Feedbacks," Climate Dynam. **24** (7–8), 2005.